FINE STRUCTURE AND MORPHOGENIC MOVEMENTS IN THE GASTRULA OF THE TREEFROG, *HYLA REGILLA*

PATRICIA C. BAKER, Ph.D.

From the Department of Zoology, University of California, Berkeley, California. Dr. Baker's present address is Department of Pathology, University of Oregon Medical School, Portland, Oregon

ABSTRACT

The blastoporal groove of the early gastrula of the treefrog, *Hyla regilla*, was examined with the electron microscope. The innermost extension of the groove is lined with invaginating flask- and wedge-shaped cells of entoderm and mesoderm. The distal surfaces of these cells bear microvilli which are underlain with an electron-opaque layer composed of fine granular material and fibrils. The dense layer and masses of vesicles proximal to it fill the necks of the cells. In flask cells bordering the forming archenteron the vesicles are replaced by large vacuoles surrounded by layers of membranes. The cells lining the groove are tightly joined at their distal ends in the region of the dense layer. Proximally, the cell bodies are separated by wide intercellular spaces. The cell body, which is migrating toward the interior of the gastrula, contains the nucleus plus other organelles and inclusions common to amphibian gastrular cells. A dense layer of granular material, vesicles, and membranes lies beneath the surface of the cell body and extends into pseudopodium-like processes and surface undulations which cross the intercellular spaces. A special mesodermal cell observed in the dorsal lining of the groove is smaller and denser than the surrounding presumptive chordamesodermal cells. A long finger of cytoplasm, filled with a dense layer, vesicles and membranes, extends from its distal surface along the edge of the groove, ending in a tight interlocking with another mesodermal cell. Some correlations between fine structure and the mechanics of gastrulation are discussed, and a theory of invagination is proposed, based on contraction and expansion of the dense layer and the tight junctions at distal cell surfaces.

INTRODUCTION

The ordered movement of embryonic cells in gastrulation has long been a subject for speculation and investigation. In the last sixty years various experimental approaches have been taken, some reviewed below, in an attempt to understand the correlative movements of gastrulation as well as the role of individual cells. These studies show that one group of cells initiate gastrulation, namely the flask or bottle cells of the entoderm, which by directional movement cause an initial insinking, the blastoporal groove, that is deepened by further invagination of these cells. The flask cells have also been thought to exert a pulling force on the involuting mesodermal cells by means of a surface coat covering all exterior cells of the gastrula. It was hoped that by observing the ultrastructure of the invaginating cells some new insight might be gained into the old problem of the mechanics of morphogenic movements.

MATERIALS AND METHODS

Pregastrular stages of the Pacific Treefrog, *Hyla regilla* (Baird and Girard), were collected from ponds in the Berkeley hills and stored at 4°C. The embryos were

removed from the refrigerator and allowed to develop to early gastrular stages (Figs. 1 *A* and 8 *A*) at room temperature. The dorsal half of the gastrula, including the blastopore and part of the future yolk plug, was isolated in Niu-Twitty solution (30). The operation was performed with a hair loop and fine glass needle on the smooth surface of a wax-lined petri dish. Great care was taken to cut the embryo cleanly and to avoid stretching or damaging the cells.

The specimens were then fixed for 1 to 2 hours at 4°C in Dalton's solution (7) adjusted to pH 7.4 with potassium hydroxide. The samples were quickly dehydrated in acetone using Parson's method (31) and flat-embedded in Epon (28). The block of plastic was trimmed so that only the blastoporal area was sectioned. Excising the dorsal half of the embryo, rather than the blastoporal region alone, not only reduced possible operative damage to the blastoporal cells, but facilitated orientation of the specimen.

Sections less than 100 mμ in thickness were cut with a glass knife and stained with lead citrate (33) for 20 to 30 minutes. The electron micrographs were made with an RCA EMU-3G.

OBSERVATIONS

The blastoporal cells have a striking appearance in electron micrographs. Their exterior surfaces and necks are elaborately structured—densely packed with cytoplasmic particles or filled with membranes, vesicles and vacuoles. This feature contrasts markedly with that of other cells of the gastrula which are largely undifferentiated and in which cytoplasmic organelles are just beginning to increase in number and complexity and in which the most prominent inclusions are yolk, lipid droplets, and cytoplasmic particles (1, 13, 22). Observations were made on the early gastrula, Stage 10 of Shumway (37). For convenient reference, early Stage 10 is divided into Stages 10A and 10B; in Stage 10A the blastoporal groove is shorter than that in Stage 10B (compare Figs. 1 *A* and 8 *A*).

Early Invagination—Stage 10A

At Stage 10A (Fig. 1 *A*) the blastoporal groove in sagittal section has the appearance of a U with long arms (Figs. 1 *B* and 1 *C*), the base of the U corresponding to the deepest extension of the blastoporal groove. The cells lining the groove in this early period may assume one of several shapes (Fig. 1 *C*): (1) flask shape with long, narrow neck distally and roughly spherical body proximally, (2) wedge shape with convoluted exterior surface, and (3) cuboidal shape with a surface which usually is smooth, but which may bear microvilli in those cells near the deepest part of the groove.

The flask-shaped blastoporal cells are found at the base of the U with their necks oriented perpendicular to the blastoporal cavity (*fc*, Figs. 1 *C* and 2). They are mostly presumptive entoderm, although some mesodermal cells may become flask-shaped as they reach the deepest extension of the groove (16). The wedge-shaped cells of the entoderm and mesoderm are found to either side of the flask cells (*wc*, Fig. 1 *C*). The cube-shaped cells are characteristic of the involuting mesoderm on the dorsal arm of the U and of the entoderm on the ventral arm.

1. Flask Cells

Parasagittal sections of the blastoporal crescent reveal flask cells with very long stalk-like necks at the base of the U (*fc*, Fig. 2). A given neck may reach a length exceeding 40 μ while being only 0.3 to 2.0 μ in width. As one continues parasagittal sectioning toward the median plane of the embryo, flask cells with shorter, broader necks (*fc*, Fig. 5) replace the long-necked cells. The number of flask cells increases until, in a saggital section of the blastoporal groove, the necks of as many as ten flask cells border on the base of the U (Fig. 6).

FIGURE 1 *A* Early gastrula at Stage 10A with blastoporal groove just beginning.

FIGURE 1 *B* Sagittal section of Stage 10A. Flask and wedge cells may be seen bordering the blastoporal groove; the cavity is the blastocoel.

FIGURE 1 *C* Drawing from large montage of electron micrographs of a parasagittal section of blastoporal groove at Stage 10A. The groove (*bg*) has the appearance of a U, with the base of the U being the innermost extension of the groove. Long-neck flask cells (*fc*), wedge cells (*wc*), and cuboidal cells (*cc*) line the groove. The distal surface of these invaginating cells contains a dense layer (*dl*) and a vesicular layer (*vl*). Note the polymorphous lipid droplets (*pl*) peculiar to invaginating cells at Stage 10A. *er*, endoplasmic reticulum; *m*, mitochondria; *mv*, microvilli; *pg*, pigment granules; *y*, yolk platelets.

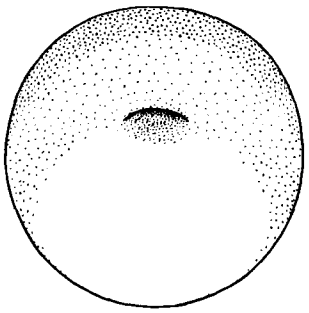

Fig. 1A

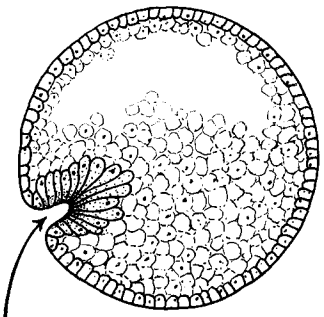

Fig. 1B

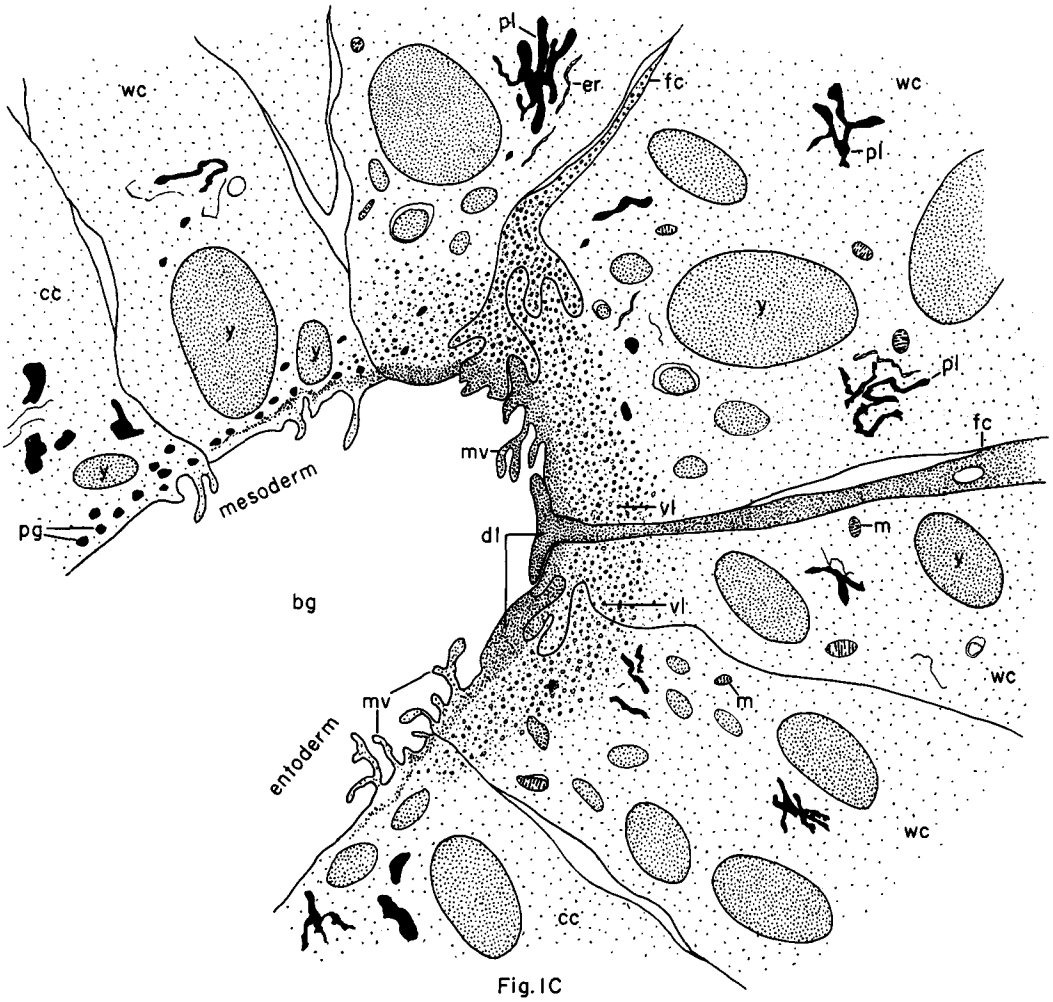

Fig. 1C

The flask cells have long microvilli on their exterior surfaces (Figs. 4 to 7). These projections contain fine cytoplasmic particles and a few vesicles, but no pigment, yolk, lipid, or other inclusions. In flask cells with extremely long necks (Figs. 2 and 4), both microvilli and necks are filled with the same dense granular substance. The microvilli adhere, along part or all of their length, to the surface of adjacent cells, forming an overlapping lip (*fl*, Figs. 2 and 4).

In the shorter, broader flask cells the microvilli are filled with particles 30 to 40 mμ in diameter (*g*, Fig. 7), which are presumably glycogen granules (12). Occasionally, a vesicle is seen among the particles (Fig. 7). These shorter cells may adhere to adjacent ones at their distal surfaces by a truncated lip (compare *fl*, Figs. 4 and 5) which may fit snugly into a depression in the surface of a neighboring cell (*fl*, Fig. 5).

An electron-opaque layer, which hereafter will be referred to as the dense layer, varying in thickness from 0.08 to 1.5 μ extends in a band beneath the cell surface of all the cells of the blastopore at the deepest extension of the groove (*dl*, Figs. 1 *C* and 2). This layer is thinner (50 to 80 mμ) and discontinuous in cells near the exterior of the blastoporal groove. It is prominent, however, beneath the exterior surface of involuting presumptive chordamesodermal cells just as they turn under the dorsal lip (not shown in these figures). In the long flask cells (*fc*, Fig. 2) the dense layer extends into the microvilli and up the neck of the cell as far as 40 μ (*dl*, Fig. 3). At higher magnification, the substance filling the neck appears uniformly granular (Fig. 4). In the shorter, broader flask cells the dense layer may widen into a round or triangular mass (*dl*, Fig. 5). In these cells the dense layer also appears to be granular, but traces of fibrils may be seen oriented parallel to the long axis of the cell (*f*, Fig. 7).

In addition to the lip junctions mentioned earlier, the distal ends of the flask cells adhere to adjacent cells in a variety of ways. In Fig. 4 the end of the neck is complexly interdigitated on both sides with wedge cells. In Fig. 6 the edges of the cells are so interlocked as to make cell boundaries hard to distinguish. Cell membranes may be quite close together with the intercellular space filled with a dense substance (see arrows, Fig. 7). Moreover, interpretation is sometimes difficult because of folds in the cell membrane or because of tangential sections.

Beneath the dense layer, the necks of flask cells are packed with masses of vesicles (*v*, Figs. 5 to 7), which may be round or crescent-shaped with an interior matrix denser than the surrounding cytoplasm. The vesicles are interpsersed with particles 10 to 40 mμ in diameter, in the size range of ribonucleoprotein and glycogen particles (*g*, Figs. 5 and 6). In the distal part of the vesicular layer are vacuoles, some surrounded by double membranes (*vc*, Figs. 5 and 6), a few pigment granules, and some granular bodies similar to the ones seen in wedge cells in Figs. 2 and 5. At a distance of some 5 to 20 μ into the neck of the flask cells, the usual organelles and inclusions appear: yolk platelets, mitochondria, lipid droplets, and Golgi apparatus (Fig. 3). The lipid droplets in the distal parts of the flask and wedge cells at this stage are unusual in being polymorphous (*pl*, Figs. 1 *C* and 2). The lipid droplets in more proximal areas of the cells (Fig. 3). and in other cells of the gastrula at this stage are roughly spherical in shape (1).

2. Wedge Cells

The dense layer in wedge cells is not so thick as that in flask cells (Figs. 2 and 5), and it contains faint fibrils oriented parallel to the outer cell surface (*f*, Figs. 4 and 5). The microvilli are more lobular in shape and less densely packed with par-

FIGURE 2 Parasagittal section of inner extension of blastoporal groove at Stage 10A, showing arrangement of long-neck flask cell (*fc*), wedge cells (*wc*), and cuboidal cell (*cc*). The ventral side of the groove is at the top of the figure, the dorsal side at the bottom. *bg*, blastoporal groove; *dl*, dense layer; *er*, endoplasmic reticulum; *fl*, flask cell lip; *gb*, granular body; *m*, mitochondria; *mv*, microvilli; *pg*, pigment granule; *pl*, polymorphous lipid droplets; *vl*, vesicular layer; *y*, yolk platelets. × 17,000.

FIGURE 3 Part of neck of flask cell seen in Fig. 2 (*fc*), 30 μ from distal cell surface. The flask cell is bordered by proximal parts of wedge cells (*wc*). Notice the dense layer (*dl*) still present beneath the lateral cell membrane. *l*, lipid droplets; *m*, mitochondria; *v*, vesicles; *y*, yolk platelet. × 24,000.

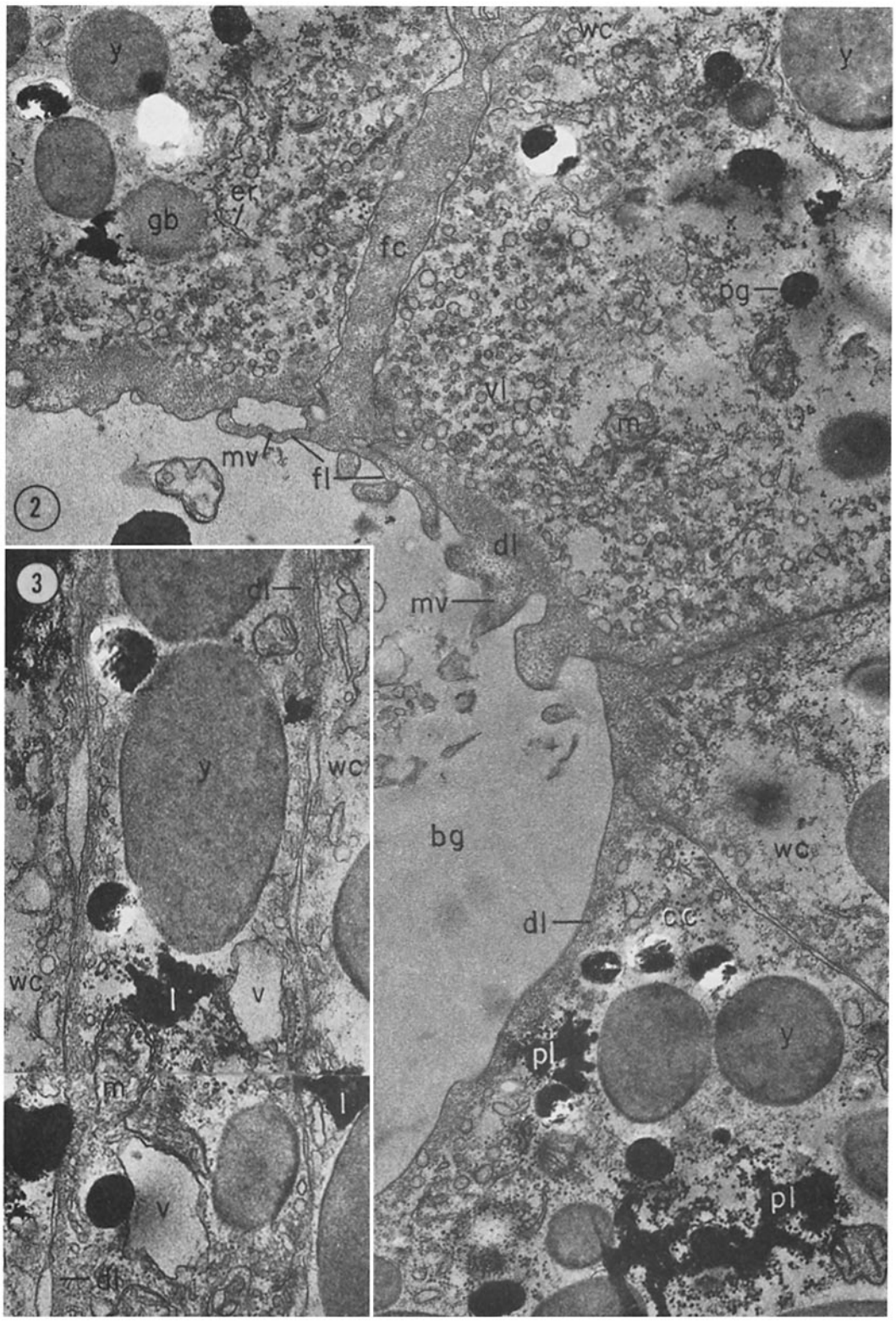
y
wc
y
er
gb
fc
pg
vl
m
mv
fl
2
dl
3
dl
mv
y
wc
bg
wc
dl
cc
wc
l
v
y
m
pl
l
v
pl
dl

ticles than those of the flask cells (Fig. 2). Whereas the vesicular layer in wedge cells (Fig. 4) has fewer vesicles and is narrower than that in flask cells (Fig. 5), the vesicles are similar in size and appearance.

The distal ends of the wedge cells are tightly joined with the same type of junctions as in flask cells: interdigitation of lateral cell membranes (Fig. 4), overlapping lips (*wl*, Fig. 5), and dense intercellular "cement" (Fig. 5). Proximally adjacent cells may be separated by intercellular spaces 20 to 80 mμ wide (Fig. 4).

Formation of the Archenteron—Stage 10B

At a slightly later period in gastrulation, the blastoporal groove assumes a longer crescent shape (compare Figs. 1 *A* and 8 *A*); sagittal and parasagittal sections of the embryo reveal that morphogenic movements of the cells have deepened and narrowed the groove (Figs. 8 *B* and *C*). The archenteron is beginning to from as a roughly spherical cavity at the anterior-most extension of the groove, *i.e.* at the base of the U seen in sectional view (Fig. 8 *C*). This cavity is bounded anteriorly by entodermal and mesodermal flask cells, dorsally by cells of the involuting mesoderm, and ventrally by flask and wedge cells of the entoderm (Figs. 8 *C* and 9). Although the gastrulating cells appear to have moved a relatively short distance in the period of time between Stages 10A and 10B, marked changes have occurred in their structure and arrangement.

1. Flask Cells

The flask cells seen at Stage 10B are presumably the same ones which initiated invagination, now augmented by a few involuting mesodermal cells converted to flask cells (16, 35, 36). By Stage 10B, the necks of the cells have shortened and become more complexly structured (compare Figs. 9 and 10 with Figs. 2 and 5). Proximally, the flask cells are now separated by wide intercellular spaces (Figs. 8 *C*, 10, and 13), across which finger-like extensions of the cytoplasm may reach from one cell to another (*p*, Figs. 10 and 13). These extensions presumably correspond to the pseudopodia formed by isolated blastoporal cells (18, 19). Although widely separated at their proximal edges, most of the flask cells are closely joined at their distal ends (Fig. 9). Some cells at the very tip of the blastopore, however, appear to have loosened their intercellular connections (see arrows, Fig. 10). As invaginating cells are known to release their connections and migrate into the blastocoel during archenteron formation (16), intercellular connections of the flask cell to the right in Fig. 10 may be loosening prior to such a migration.

The microvilli on the surface of the cells now appear thinner and longer than in Stage 10A, and they are filled with the substance of the dense layer. Again, within the granular matrix of the layer faint fibrils may be detected running parallel to the surface (*f*, Fig. 11). Whorls of membranes and stacks of vesicles are occasionally found embedded in the dense layer (Fig. 12).

Beneath the dense layer are large vacuoles enclosed by a single membrane (*vc*, Figs. 9 and 10). Some vacuoles are embedded in a network of membranes and tubules and appear to be filled with a homogeneous electron-transparent material. The masses of membranes which surround the vacuoles and continue into the cell neck are not arranged in any discernible pattern. In some areas, the membranes appear to be aggregations of vesicles (*v*, Fig. 11); other areas contain highly folded membranes (*ml*, Fig. 10) interspersed with small oblong vesicles or spaces. Farther along the neck the membranous layer gives way to lipid droplets, yolk platelets, mitochondria, pigment granules, cytoplasmic particles, and endoplasmic reticulum (Figs. 9 and 10).

The body of an invaginating cell contains the nucleus as well as the above-mentioned organelles and inclusions. Its dense cortex contains membranes and small vesicles (*mv*, *v*, Fig. 13). This layer seems a thinner version of the dense layer in the cell neck. Finger-like psuedopodia which bridge the intercellular gaps are also filled with the dense substance (*p*, Fig. 13).

Figure 4 Higher magnification of distal end of neck of flask cell in Fig. 2, showing lip (*fl*) of cell, interlocking of flask (*fc*) and wedge cells (*wc*) in region of dense layer (*dl*), and faint fibrils (*f*) in dense layer. *bg*, blastoporal groove; *v*, vesicles in vesicular layer. × 65,000.

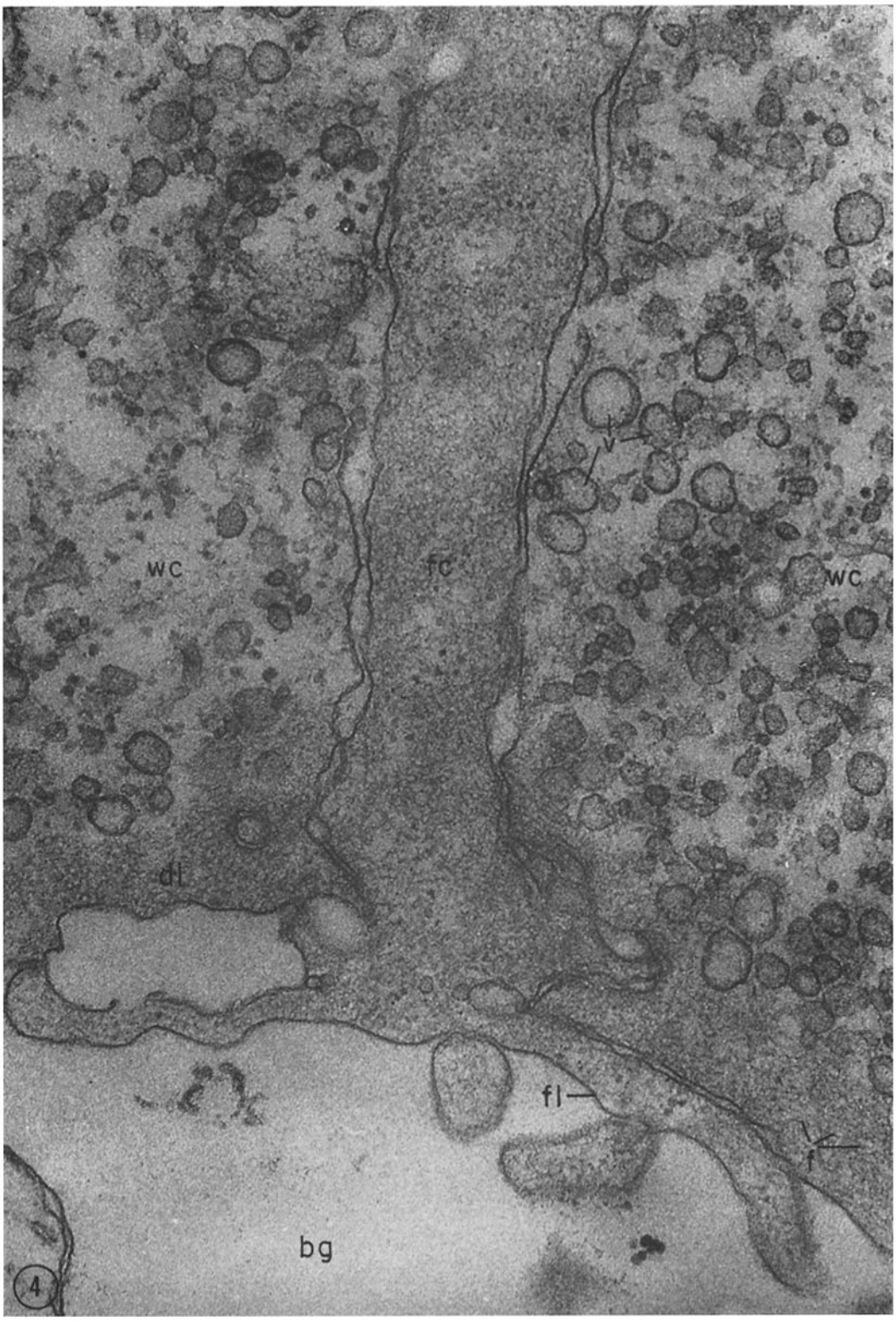
wc
fc
v
wc
dl
fl
f
bg
4

2. Wedge Cells

At Stage 10B, wedge-shaped cells are confined to the ventral entodermal lining of the archenteron and are situated slightly distal to the deepest extension of the groove (*wc*, Figs. 8 *C* and 9). The surface of the cells bordering the groove is skewed toward the base of the groove, and the microvilli are longer and more numerous than in the wedge cells of Stage 10A (compare Figs. 2 and 9). The dense layer, not so dark as in the adjacent flask cells, extends into the microvilli (Fig. 9). The cytoplasm proximal to the dense layer is filled with tubules and vesicles.

3. Involuting Mesodermal Cells

The mesodermal cells, easily distinguished because of their pigment granules, line the dorsal side of the forming archenteron and extend along the dorsal wall of the blastopore to the exterior (Figs. 8 *C* and 9). Whereas most involuting cells appear cuboidal in shape, mesodermal cells lining the forming archenteron are roughly rectangular with their long axis parallel to the arms of the U. Like the flask and wedge cells in this area, the mesodermal cells are separated by intercellular spaces 0.5 to 3 μ in width (Fig. 8 *C*); involuting mesodermal cells distal to the point *bg* on Fig. 8 *C*, however, are closely packed.

In the area of the forming archenteron, a type of cell appears among the involuting mesodermal cells which bears some resemblance to the invaginating flask cells. These special cells are smaller and denser than the surrounding mesoderm, and long fingers of cytoplasm extend from their distal surfaces along the edge of the blastoporal groove (Fig. 14). The tip of an extended finger is interlocked with cytoplasmic extensions of other elongate mesodermal cells (*cj*, Figs. 14 and 15). Proximally, the cell body adheres to adjacent mesodermal cells by pseudopodia (*p*, Fig. 14) which bridge the intercellular spaces (*i*, Fig. 14). Microvilli on the surface are filled with extensions of the dense layer; beneath the dense layer may be seen masses of membranes and vesicles. Cytoplasmic particles 15 to 40 mμ in diameter, presumably ribonucleoprotein and glycogen, may be seen in abundance in all parts of the cell (*g*, Figs. 14 and 15). Pigment granules are more concentrated than in other mesodermal cells (compare adjacent cells in Fig. 14).

DISCUSSION

History

The flask cells of the blastopore have been studied with the light microscope by many investigators (14–16, 34, 35, 38), and numerous theories have been advanced to explain their movement (see reviews in 2, 8, 16, 17, 36, 38). Vogt as early as 1929 (39) suggested that invagination was due in part to an active contraction of the distal ends of the blastoporal cells. Waddington (40) developed this idea further by speculating that the causative agent for invagination of the entoderm might be fibers of protein at the outer edge of the blastoporal cells which actively contract and reduce the distal parts of the blastoporal cells, thereby initiating invagination. In an attempt to obtain direct evidence for this theory, Picken and Waddington (40) showed that the yolk-free necks of the flask cells exhibit a weak birefringence indicating the presence of fibers running along the length of the processes and perpendicular to the outer surface of the egg. Lewis (25, 26) developed a similar theory working largely with models. He attributed invagination in *Amblystoma punctatum* to an active contraction of a "gel layer" at the outer ends of the entodermal cells.

Holtfreter (15–21) has contributed the most detailed experimental analysis of structure and movement of the blastoporal cells. He discounts the idea that contraction of cell surfaces plays a part in invagination; rather, he thinks that invagination depends on the inward migration of the blastoporal cells and on the properties of a "surface coat" covering the exterior of the embryo. The results of his work pertinent to this discussion may be summarized as follows.

The driving force initiating gastrulation is lo-

FIGURE 5 Another type of flask cell (*fc*) bordered by wedge cells at the innermost extension of the groove (Stage 10A, parasagittal section). *bg*, blastoporal groove; *dl*, dense layer; *er*, endoplasmic reticulum; *f*, fibrils in the dense layer; *fl*, flask cell lip; *g*, cytoplasmic (glycogen ?) granules; *gb*, granular body; *mv*, microvilli; *v*, vesicles in vesicular layer; *vc*, vacuole; *wl*, wedge cell lip; *y*, yolk platelet. × 33,000.


y
fc
er
gb
vc
g
dl
mv
fl
mv
bg
wl
5

cated within the flask cells of the entoderm. At the time of gastrulation, the inner parts of these cells begin to migrate inward, owing in part to some difference in milieu between the proximal and distal surfaces of the cells (*e.g.* alkalinity of the blastocoelic fluid) and partly to an inherent tendency of these cells to elongate and migrate along their proximo-distal axis. As the blastoporal cell migrates inward, by a mechanism of contraction and expansion of the cell surface, the distal part remains firmly attached to a surface coat and is drawn out into a flask shape. "When cellular deformation has reached a certain point, the tensile strength of the elastic neck portion forces the coated surface to yield and to recede into the interior in the form of the archenteron" (17). The tangential pull exerted by the invaginating blastoporal cells throughout the coat then pulls in the marginal cells.

Holtfreter (15) stated that the surface coat is a layer, under elastic tension, which surrounds the exterior of the embryo and binds the peripheral cells together into a supercellular unit, integrating their movements. In an early paper (15) he said the coat was contractile, but in a later paper (38) he stated the opposite. Holtfreter speculated that the coat either closely adhered to the cell membrane or was an actual continuation of the cytoplasm.

As a surface coat is an essential feature in Holtfreter's theory of gastrulation, various investigators have attempted to verify its existence. Dollander (9, 11) observed an extracellular coat surrounding the fertilized egg of *Triton* which stained with Nile blue sulfate, but he was unable to demonstrate such a coat in later stages (10). Løvtrup (27) stated that an extracellular coat exists in *Rana temporaria* embryos which takes part in osmoregulation by mechanically opposing osmotic swelling. Bell (5, 6) reported that a surface coat composed of mucopolysaccharides can be removed from *Rana pipiens* gastrulae and neurulae by means of focused ultrasound. Electron micrographs have not supported Holtfreter's hypothetical picture of a continuous cell covering congruent with the cytoplasm or closely amalgamated to the cell membrane. Karasaki (22) found no evidence for a surface coat in electron micrographs of ectoderm of *Triturus pyrrhogaster* embryos ranging in age from early blastula to late tail-bud, nor did Matsumoto (29) who examined neural plate cells and cells of the blastoporal groove in the same species. The electron micrographs of the blastoporal groove in the frog *Phrynobatrachus natalensis* (3) reveal no extracellular covering or coat.

Structure of the Blastoporal Cells

The present study, in agreement with the studies on *Triturus* and *Phrynobatrachus*, shows no evidence of a surface coat. It may be possible that an extracellular mucopolysaccharide coat, such as that seen in the light microscope surrounding fertilized eggs (9) or removed by ultrasound (5), is present but not discernible by fixation methods used in electron microscopy. It is doubtful, however, that such a covering plays a direct part in morphogenic movements. It is hard to imagine a covering, closely adhered to the cell surface and under elastic tension, which could be penetrated by the long, wavy microvilli seen in Figs. 2, 5, and 6 or which would allow the irregularity of cell surfaces seen in Fig. 9. Presumably, the exterior cell surface is thrown into microvilli as the cuboidal cells change to wedge and then flask cells. The microvilli are longest in the cells whose distal surface is most compressed. Compare the microvilli (*mv*) in flask (*fc*) and adjacent wedge cell (*wc*) with the surface of a cuboidal cell (*cc*) in Fig. 2.

My findings support those of Holtfreter (16) that a long stalk-like neck is characteristic of flask cells in earliest invagination; these cells are found in Stage 10A, but not in Stage 10B. The necks of the

FIGURE 6 Flask cells at base of U in sagittal section of blastoporal groove (Stage 10A). Sections are from the same specimen as that shown in Fig. 2. Notice the interlocking of cell membranes. *bg*, blastoporal groove; *dl*, dense layer; *g*, cytoplasmic (glycogen?) granules *mv*, microvilli; *v*, vesicle of vesicular layer; *vc*, vacuole. × 26,000.

FIGURE 7 Higher magnification of flask cells at base of U in sagittal section. Arrows point out tight cell adhesions with a dense substance or "cement" between the cell membranes. Note fibrils (*f*) in the dense layer (*dl*). *bg*, blastoporal groove; *g*, cytoplasmic (glycogen ?) granules; *mv*, microvilli; *v*, vesicles in vesicular layer and one in a microvillus. × 67,000.

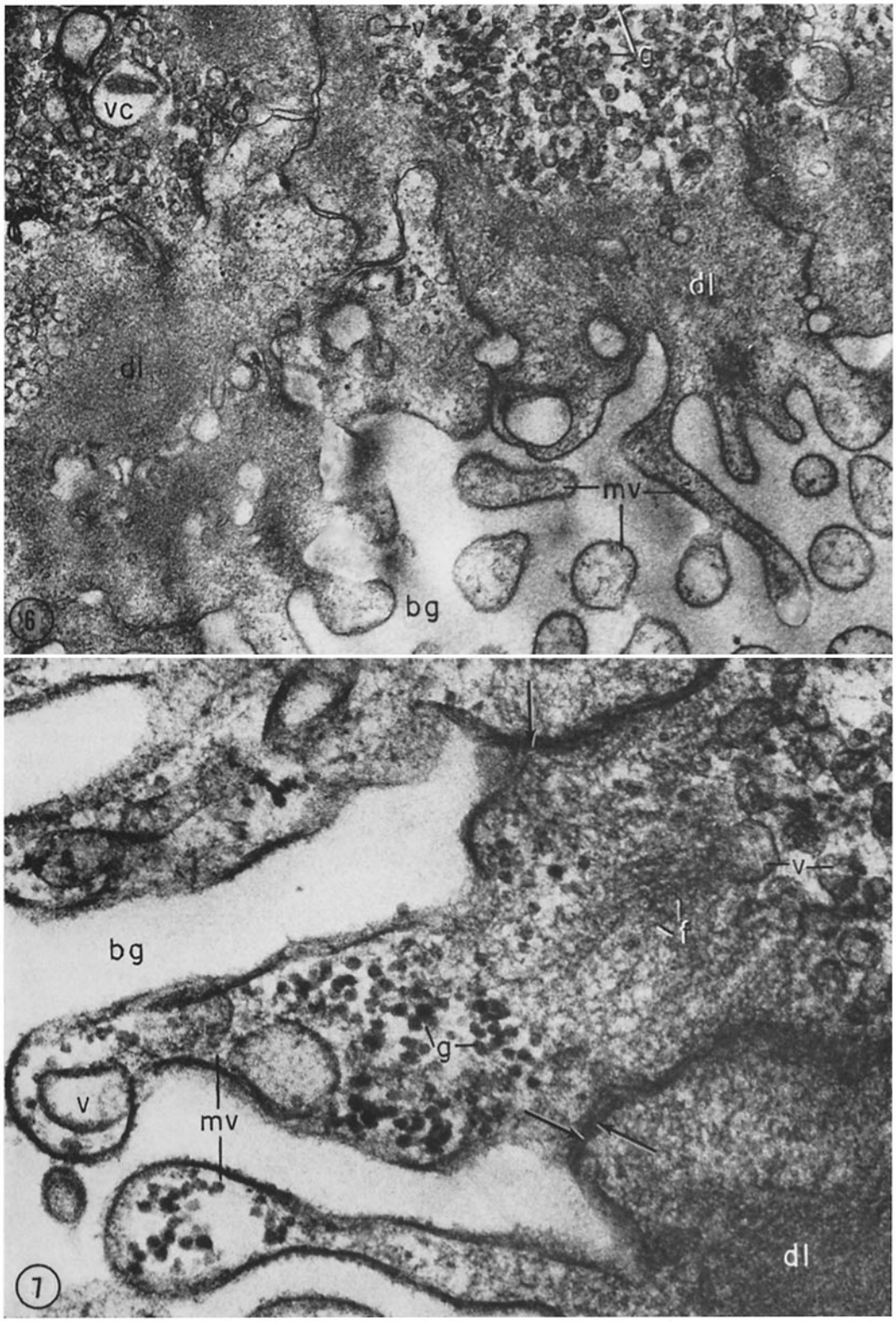
v
g
vc
dl
dl
mv
bg
6
bg
v
f
g
v
mv
dl
7

flask cells appear quite dark in light micrographs. This was thought to be due to heavy pigmentation of these regions (16, 26, 36), but the electron microscope reveals that the opacity is due to densely packed particles, membranes, and vesicles in the necks and distal ends of the flask cells (Figs. 2, 5, 9, and 10), and not to pigment granules.

The general structure of the central part of the blastoporal pit in *Phrynobatrachus natalensis* (3) resembles the same area in *Hyla regilla* (Fig. 6); the necks of flask cells, bearing long microvilli, crowd the base of the groove. Balinksy did not observe the long-necked flask cells seen in Figs. 2 and 5, presumably because his sections were from the sagittal plane of the blastoporal crescent. He observed no dense layer or vesicular layer comparable to that seen in Figs. 5 and 6. The blastoporal cells in *Phrynobatrachus* appear to be tightly joined at their outermost edges; often the cell membranes are more electron-opaque in these regions. Balinsky thinks that the electron-opaque substance may be a cement. I agree with his interpretation that the adhesion of cells at their distal surfaces, whether by "cement" (arrows, Fig. 7) or by interlocking (Figs. 4, 6, and 15), could account in part for the integrated mass movements of involuting cells.

Although Balinsky (3) did not observe a dense layer beneath the blastoporal cell surface in the very early gastrula of *Phrynobatrachus*, his micrographs show a band of particles 0.08 to 0.2 μ wide beneath the microvilli of cells in the middle of the neural plate. He postulates that this band is a contractile layer which is responsible for the wedge shape of the neural plate cells. Matsumoto's (29) electron micrographs of early Stage 12 gastrulae of *Triturus pyrrhogaster* show a dense band, 25 to 60 mμ wide, composed of microparticles beneath the microvilli of involuting mesodermal cells inside the blastoporal groove (the exact location of the cells is not made clear). A similar layer 150 to 200 mμ in thickness is seen beneath the cell membrane in his micrographs of the middle part of the neural plate in Stage 19 embryos. Karasaki (22) reported a dense layer at the base of the microvilli in electron micrographs of neural ectoderm in *Triturus pyrrhogaster* at Stage 14. Neither Matsumoto nor Karasaki speculates on the function of this layer. The dense bands described in the literature resemble the dense layer seen in my micrographs. In all cases, the band is composed of closely packed particles and lies beneath the microvilli at the distal cell surface. The layer seems to present a barrier to cellular inclusions, and has been found only in flask and wedge cells of the embryo undergoing morphogenic movement. Only in *Hyla* were fibrils seen in the dense layer (Figs. 5, 7, and 11). This may be because the earlier micrographs of Balinsky, Karasaki, and Matsumoto were not of sufficient resolution or magnification to reveal fibrils if present.

Holtfreter (16) observed that, as invagination proceeds and the blastopore becomes deeper, more and more wedge cells are transformed into flask cells, taking the place of flask cells which have migrated into the interior cell mass or into the blastocoel. Some of the wedge cells seen in Fig. 2 probably represent intermediate forms in the conversion of an involuting mesodermal or entodermal cell into a flask cell. As the neck narrows and lengthens, the dense layer widens and the vesicles become

FIGURE 8 *A* Stage 10B with blastoporal crescent slightly more pronounced than in Stage 10A (Fig. 1 *A*).

FIGURE 8 *B* Sagittal section of Stage 10B. The blastoporal groove has lengthened, and the archenteron (arrow) is beginning to form at the inner end of the groove.

FIGURE 8 *C* Drawing from large montage of electron micrographs of inner extension of blastoporal groove in sagittal section of Stage 10B. The archenteric cavity (*ac*) is beginning to enlarge. The entodermal flask (*fc*) and wedge cells (*wc*) forming the ventral lining of the archenteron are seen in longitudinal section. The anterior end of the archenteron is lined by flask cells of the entoderm and mesoderm, some cut in cross-section. Roughly rectangular and cuboidal mesodermal cells form the dorsal roof of the archenteron. Note the large intercellular spaces (*i*) bridged by pseudopodium-like process (*p*) between cells, and the specialized mesoderm cell (*sm*) with a dense cytoplasmic finger extending along the surface of the involuting mesoderm. *bg*, blastoporal groove; *l*, lipid droplets; *m*, mitochondria; *ml*, membranous layer; *vc*, large vacuoles in flask cells; *y*, yolk platelets.

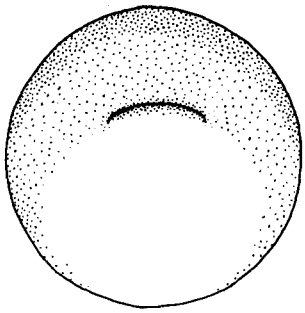

Fig. 8A

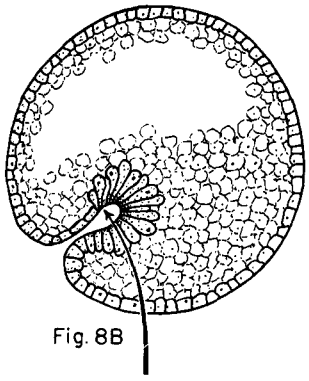

Fig. 8B

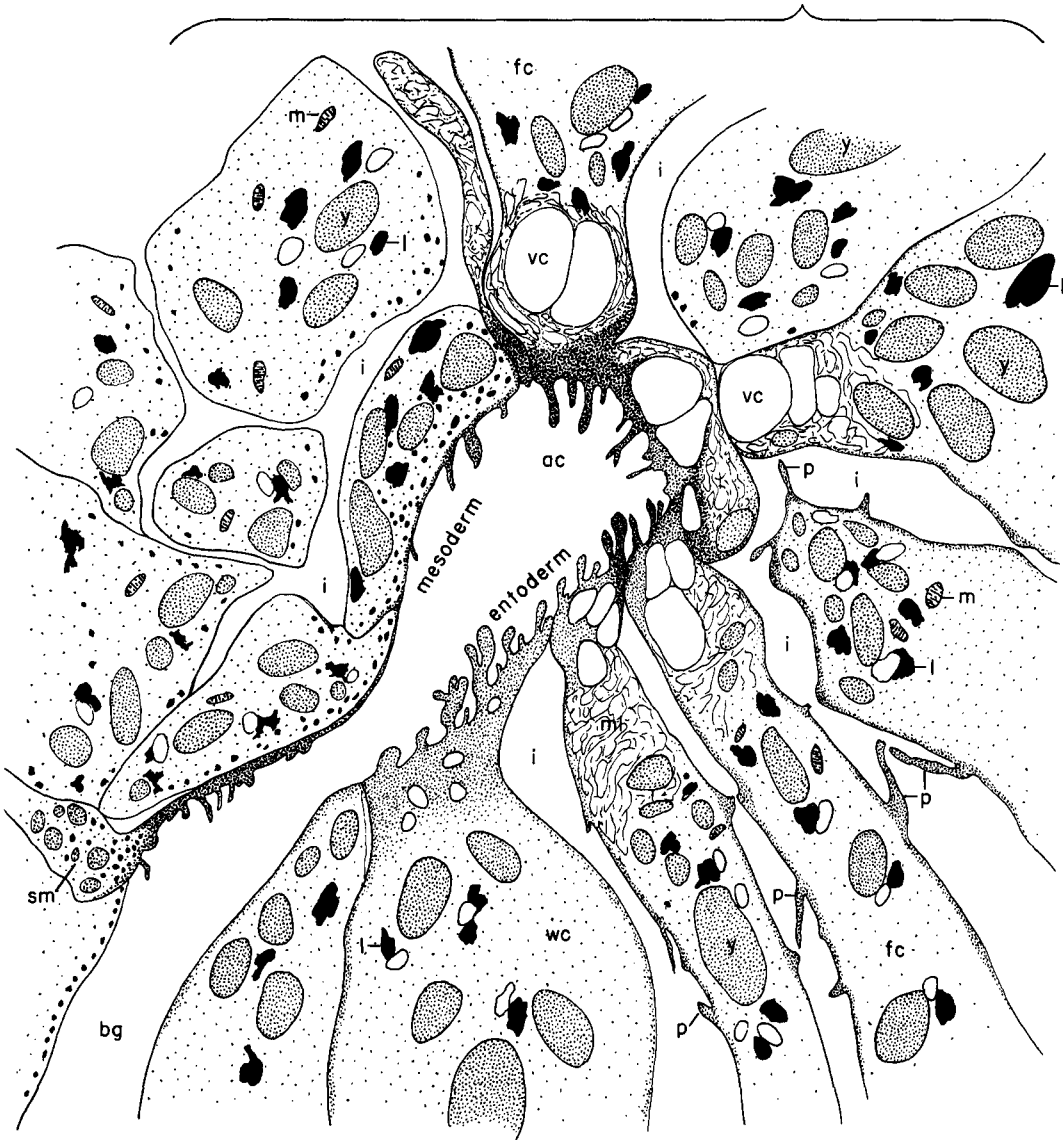

Fig. 8C

tightly packed in the cell neck. The other inclusions are displaced proximally. It is possible that the vesicles at Stage 10B coalese as the neck retracts to form the membranous layer seen at Stage 10B. The vesicular layer, like the dense layer, is found only in those gastrular cells involved in morphogenic movements. It is likely that the vesicles of Stage 10A and the membranes of Stage 10B are elements of the endoplasmic reticulum involved in synthesis of the dense layer. This will be discussed in more detail in a later paper.

The large vacuoles in the necks of the flask cells lining the archenteron may have an excretory or secretory function. The shortening and retracting of the cell neck, which is presumably occurring in those flask cells retreating into the interior (16), could be accomplished, in part, by an excretion of fluids from the cytoplasm of the cell neck. Or the vacuoles may be pinocytotic. Balinsky and Walther (4) have observed large vesicles in flask cells of the primitive streak in the chick; they presume the vesicles to be pinocytotic, but they do not comment on the significance of such a process.

Holtfreter (17) was unable to explain what happened to the blastocoelic fluid when the archenteric cavity replaced the blastocoel, as the coat covering the cells of the archenteron was relatively impermeable to water. In the light of the present study it would seem that, as some of the flask cells release their connection distally and retract into the interior, a temporary canal is opened into the archenteron (see arrows, Fig. 10) which, in the absence of a coat, would allow blastocoelic fluid under pressure from the invaginating cell mass to pass into the archenteric cavity.

Mechanics of Gastrulation

Conclusions concerning dynamic processes drawn from studies of cell structure must be tentative, but the preceding micrographs suggest support for some of the theories which have been advanced to explain morphogenic movements. The contractile band mechanism proposed by Balinsky (3) for neurulation can now be postulated for gastrulation. The dense layer also offers a structure for Waddington's (40) predicted mechanism of gastrulation (*i.e.*, fibers or a protein matrix which could undergo "fibrisation" and by contraction and expansion cause morphogenic movements), as well as a mechanism for contraction and expansion of the proximal cell surface (19–21). If we assume that the dense layer undergoes contraction and expansion, then invagination (*i.e.*, insinking, blastoporal groove formation, and subsequent archenteron formation) could be accomplished by the flask and wedge cells in a twofold manner: alternate shortening and elongation of the dense layer in the neck and distal ends of the cells, and migration of the inner ends of the cells by periodic contraction and expansion of the dense layer beneath the outer cell surface. In the following discussion, reference will be made to the line diagram in Fig. 16 which offers a hypothetical scheme for the action of flask cells in gastrulation.

Whether initial inpocketing of the entoderm is caused by a contraction of the dense band or by a pull exerted by the migrating proximal ends, or both, is unknown. I have not observed the first stages of invagination. Balinsky's micrographs (3) of what is probably an earlier stage than my Stage 10A do not reveal a dense layer in the blastoporal cells, which suggests that the initial insinking may be due to migration alone. By the time the blastopore appears as a distinct crescent (Fig. 1 *A*), however, the dense layer is present beneath the surface of the cells lining the anterior-most extension of the blastopore and in the long necks of the flask cells (Fig. 2). A contraction of the dense layer in a plane parallel to the cell surface (Fig. 2) would narrow the ends of the cells and deepen the blastoporal groove (*b* and *c*, Fig. 16). A contraction of the long neck in a plane perpendicular to the distal cell surface would further deepen the groove (*e* and *f*, Fig. 16).

Although action in the neck may be partially responsible for invagination, the main inward pull is exerted by the migrating proximal ends of the cells (16–19, 38). Such a pull presupposes an

FIGURE 9 Archenteric cavity (*ae*) forming at inner end of blastoporal groove in Stage 10B, lined dorsally by mesoderm, ventrally by entoderm, and anteriorly by flask cells (*fc*) of mesoderm and entoderm. (See Fig. 8 *C*). *dl*, dense layer; *gb*, granular body; *i*, intercellular space; *l*, lipid droplets; *mv*, microvilli; *pg*, pigment granule; *vc*, vacuoles in flask cells; *wc*, wedge cell; *y*, yolk platelets. × 5,000.

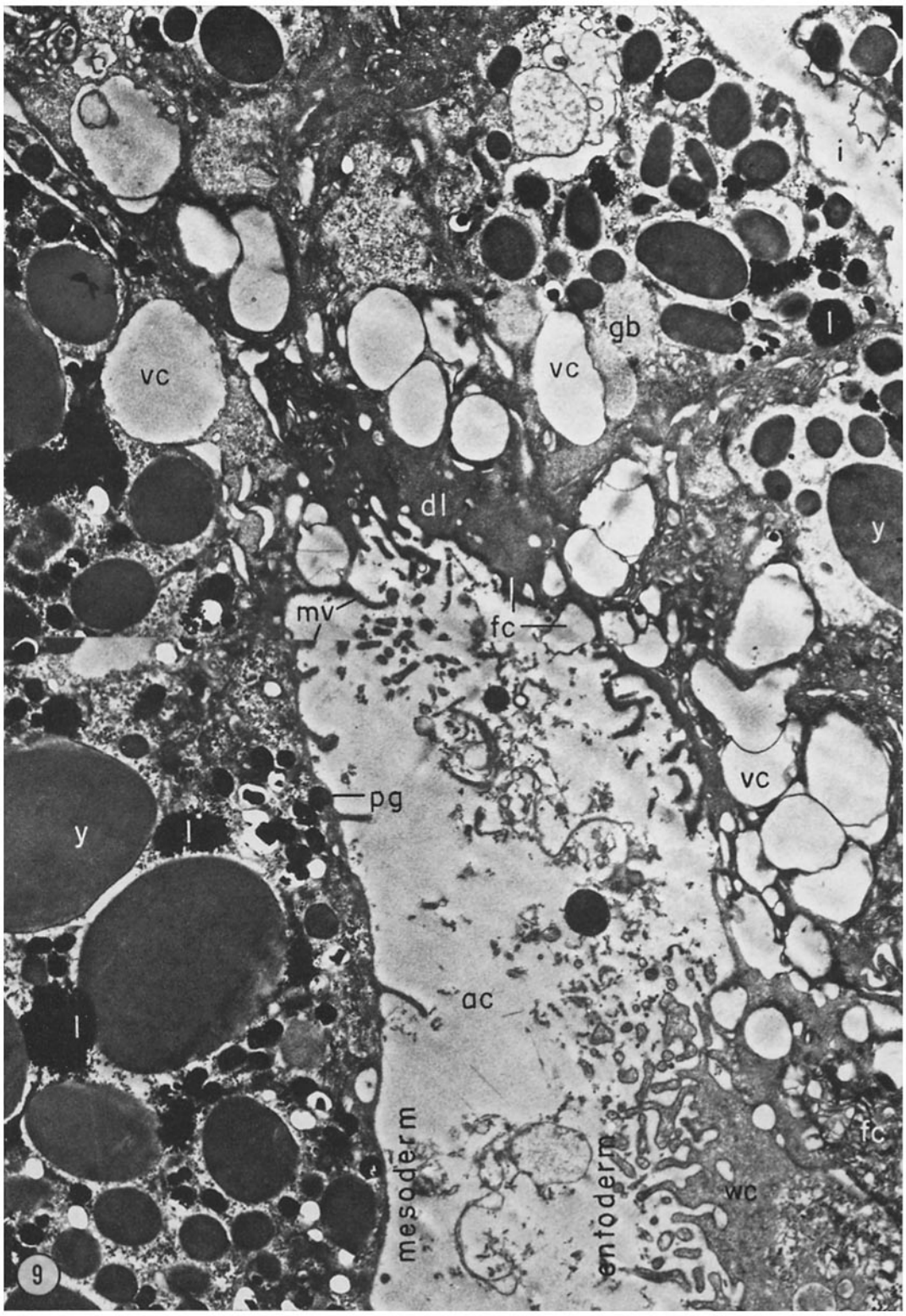
i
gb
vc
vc
dl
y
mv
fc
vc
pg
y
l
ac
l
mesoderm
entoderm
fc
wc
9

anchoring of the cell surface in some way. The arrows in Fig. 13 may point out cellular adhesions at the tips of microvilli and at surface undulations. Recently Lesseps (24) has shown that reaggregating heart and pigmented retinal cells in the chick embryo make initial contact at the crests of surface undulations or at the tips of pseudopodium-like processes. He suggests that these protrusions function to reduce the repulsive force between approaching cells, allowing the formation of adhesive bonds which can then expand over a broader area. Such bonding may occur temporarily in the blastoporal cells, giving the cell traction as it moves inward.

After extensive experimental work on isolated embryonic cells, Holtfreter (19, 20) concluded that they do not move by sol-gel transformations supposedly responsible for amoeboid locomotion, but by alternating contractions and expansions of the cell surface. In the blastoporal cells this "three-steps-forward, two-steps-backward" succession of movements is confined to the inner end, resulting in a net movement toward the interior. The question immediately arises as to how the structure of the cell surface of a migrating blastoporal cell compares to pseudopodia of an ameba. In contrast to the highly structured migrating end of the blastoporal cell, electron microscopy has revealed little structure in the moving areas of cytoplasm in amoebae (32). Electron micrographs of Wohlfarth-Botterman (41, 42) show a lightly granular cytoplasm in pseudopodia which presumably were moving at the time of fixation, and Lehmann (23) has shown the presence of a fibrous material beneath the plasmalemma of *Amoeba proteus*.[1] The pseudopodia of reaggregating heart and retinal cells in the chick are also filled with a substance denser than the cell cytoplasm (24). One may speculate, then, that migration of the proximal ends of cells occurs in the following way. The dense layer expands to form projections of the cell surface which temporarily anchor to other cells (*p* and arrows, Fig. 13). The dense layer then contracts. If the net movement forward owing to expansion exceeds the net movement backward owing to contraction, the result will be the "three-steps-forward, two-steps-backward" movement described by Holtfreter (19, 20, 38) in isolated blastoporal cells. New pseudopodia expand and adhere, and the flask cell continues to move inward, deepening the blastoporal groove. The net inward movement of the proximal end is represented by the longer dashed arrows in Fig. 16.

Because of tight junctions between adjacent cells, the movement of the flask cells would account, in part, for the coordinated movements of involuting cells. As the invaginating cells contract distally and migrate inward they drag their neighbors behind them, just as if they were attached to a supracellular covering. This passive movement is not the whole story of involution, however, as the chordamesodermal cells have been shown to have self-stretching tendencies (16, 25, 36), and the special mesoderm cell seen in Fig. 14 may play an active role in involution. It is possible that contraction and expansion of the dense layer in the long finger of the cell pulls adjacent mesodermal cells toward the interior of the embryo.

The question remains as to the mechanism by which the dense layer contracts. Presumably, the layer is made up of a proteinaceous matrix interspersed with protein fibers; whether the matrix or the fibers undergo contraction is a matter for spec-

[1] *Note added in proof:* Since acceptance of this manuscript for publication, electron micrographs have been published demonstrating the presence of a dense matrix and thread-like or fibrillar elements in the moving portion of the ground plasm of the amoeba *Hyalodiscus simplex*, *Amoeba proteus*, and the slime mold *Physarum* (43). This morphological evidence adds support to the contractility theory of amoeboid movement.

FIGURE 10 Higher magnification of neck of flask cells at anterior surface of archenteron (*ac*). Presumably these cells, the same ones which initiated insinking of the blastopore, have reached the limits of invagination and are retracting into the interior. Arrows mark the loosening of distal connections. Pseudopodium-like processes (*p*), which may anchor the migrating cell, cross intercellular spaces (*i*). The vesicular layer seen in Figs. 5 and 6 is replaced by a membranous layer (*ml*) which surrounds large vacuoles (*vc*). The characteristic dense layer (*dl*) extends into the microvilli (*mv*). Proximal to the membranous layer the cell neck contains granular bodies (*gb*), lipid (*l*), mitochondria (*m*), and yolk platelets (*y*). × 17,000.


gb
i
l
m
p
y
i
ml
ml
vc
vc
dl
mv
dl
10
ac

ulation. It is hoped that better methods of fixation combined with experimental work on isolated flask cells will assist in the solution of these problems. The theory of a contracting and expanding dense layer offers, of course, only a partial explanation of the mechanics of gastrulation. Nothing is known about why the flask cells begin invagination, what establishes their axial polarity, or what determines which cells will elongate.

This paper is a section of a thesis submitted in partial fulfillment of the requirements for the Ph.D. degree.

Grateful acknowledgement is made to Prof. Richard M. Eakin for his generous and invaluable assistance in preparing this paper for publication, to Prof. William E. Berg for a critical reading of the manuscript, to Mrs. Emily E. Reid for the drawings, and to the United States Public Health Service for fellowship support.

Received for publication, Feb. 10, 1964.

REFERENCES

1. BAKER, P. C., Changes in lipid bodies during gastrulation in the treefrog, *Hyla regilla*, *Exp. Cell Research*, 1963, **31**, 451.
2. BAKER, P. C., Ultrastructure of the gastrula of *Hyla regilla*, Doctoral thesis, University of California, Berkeley, 1964.
3. BALINSKY, B. I., Ultrastructural mechanisms of gastrulation and neurulation, *in* Symposium on Germ Cells and Development, Institut International d'Embryologie and Fondazione A. Baselli (1960), Pallanza, 1961, 550.
4. BALINSKY, B. I., and WALTHER, H., The immigration of presumptive mesoblast from the primitive streak in the chick as studied with the electron microscope, *Acta Embryol. et Morphol. Exp.*, 1961, **4**, 261.
5. BELL, E., Dissociation of ectodermal cells and of the "surface coat" from amphibian embryos by means of focused ultrasound: the character of the "surface coat," *Anat. Rec.*, 1958, **131**, 532.
6. BELL, E., Some observations on the surface coat and intercellular matrix material of the amphibian ectoderm, *Exp. Cell Research*, 1960, **20**, 378.
7. DALTON, A. J., A chrome-osmium fixative for electronmicroscopy, *Anat. Rec.*, 1955, **121**, 281.
8. DEHAAN, R. L., Cell migration and morphogenetic movements, *in* The Chemical Basis of Development, (W. D. McElroy and B. Glass, editors), Baltimore, The Johns Hopkins Press, 1958.
9. DOLLANDER, A., Observations concernant la structure du cortex de l'oeuf de certains amphibiens urodèles mise en évidence du "coat" de Holtfreter, *Compt. rend. Assoc. Anat.*, 1951, **38**, 430.
10. DOLLANDER, A., Observations relatives a certaines propriétés du cortex de l'oeuf d'amphibien, *Arch. Anat. Micr. et Morphol. Exp.*, 1953, **42**, 185.
11. DOLLANDER, A., La structure du cortex de l'oeuf de Triton observée sur coupes fines et ultrafines au microscope ordinaire, et au microscope électronique, *Compt. rend. Soc. biol.*, 1954, **148**, 152.
12. EAKIN, R. M., Actinomycin D inhibition of cell differentiation in the amphibian sucker, *Z. Zellforsch.*, 1964, in press.
13. EAKIN, R. M., and LEHMANN, F. E., An electro-

FIGURE 11 Distal surface of flask cell of Stage 10B at higher magnification to show part of membranous layer (*ml*), vesicles (*v*), vacuoles (*vc*) surrounded by a single membrane, and faint fibrils (*f*) in granular matrix of dense layer (*dl*). × 48,000.

FIGURE 12 Part of distal surface of flask cell at Stage 10B showing whorls of membranes (*m*) and vesicles (*v*) or cross-sections of tubules embedded in the dense layer (*dl*). *vc*, vacuole. × 46,000.

FIGURE 13 Parts of migrating inner ends of several adjacent flask cells at Stage 10B. The pseudopodium-like processes (*p*) which cross the intercellular spaces (*i*) may adhere temporarily to adjacent cells (arrows) serving as an anchor for the invaginating flask cell. The mechanism for movement may reside in the structure of the granular matrix, vesicles (*v*), and membranes (*mv*) which make up the dense layer (*dl*); *gb*, granular body; *l*, lipid droplet; *m*, mitochondria; *y*, yolk platelets. × 21,000.

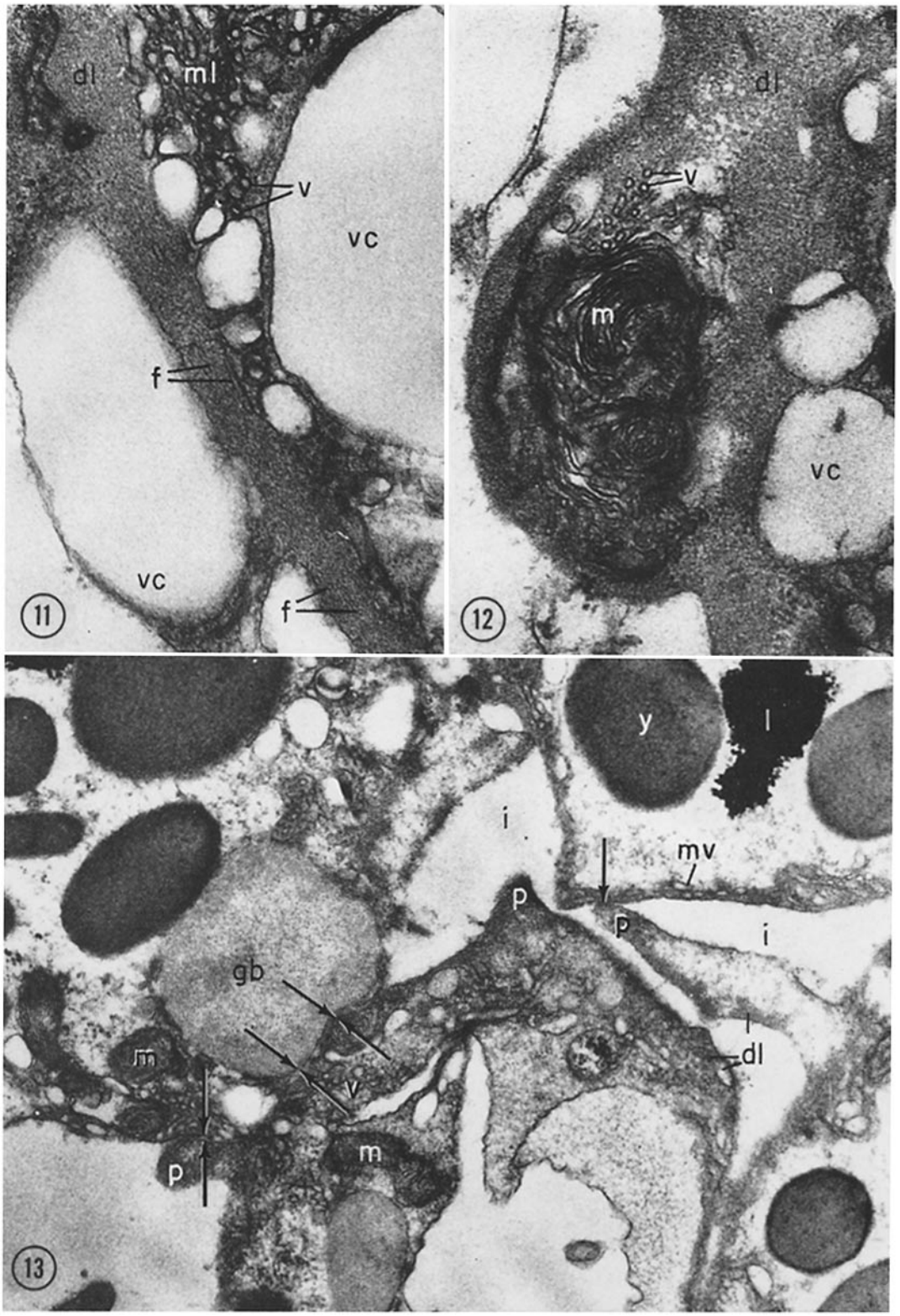
dl
ml
v
vc
f
vc
f
11
dl
v
m
vc
12
y
l
i
mv
p
p
i
gb
m
v
dl
m
p
13

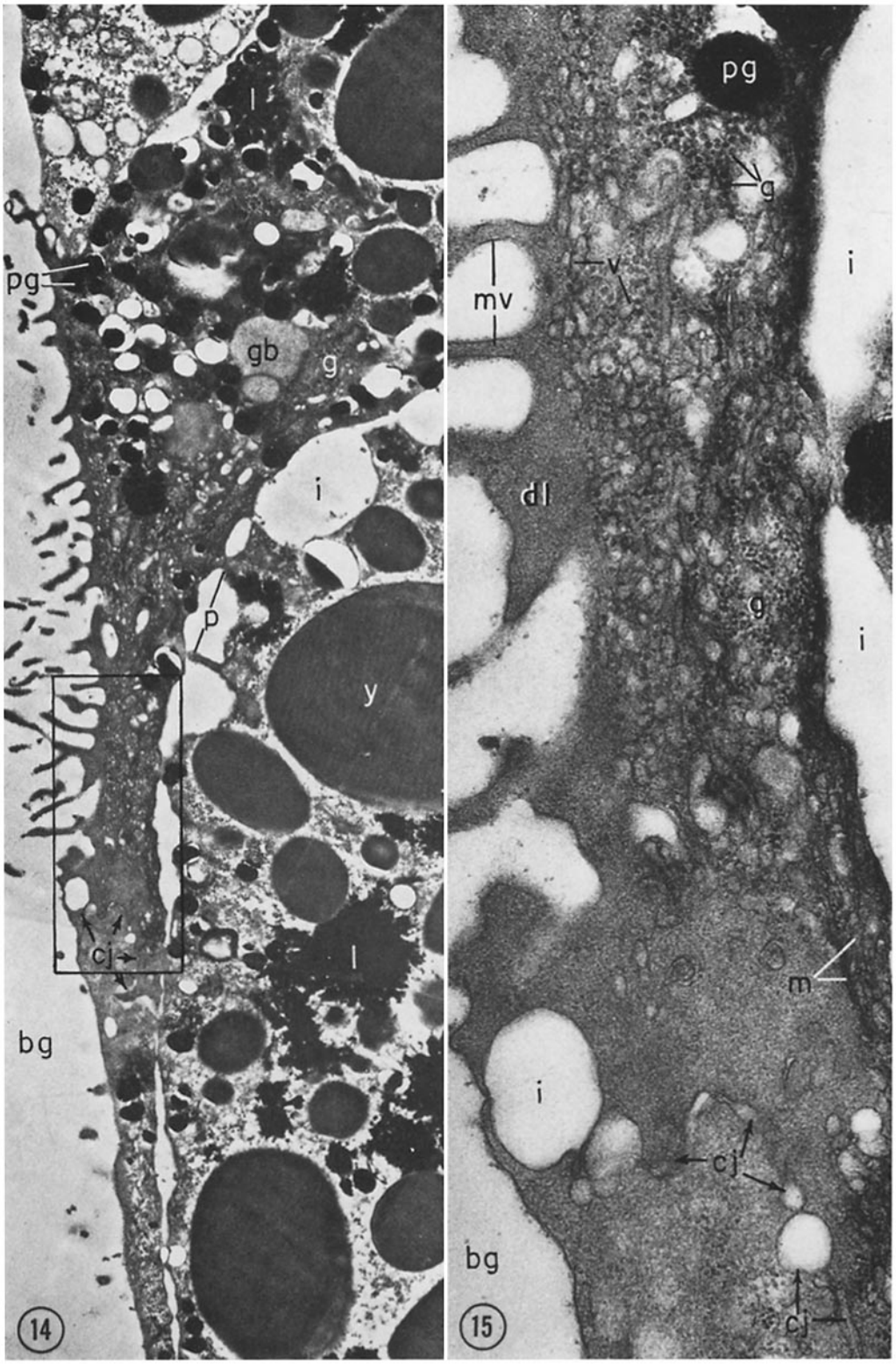
l
pg
gb
g
i
p
y
cj
l
bg
14
pg
g
v
mv
i
dl
g
i
m
i
cj
bg
cj
15

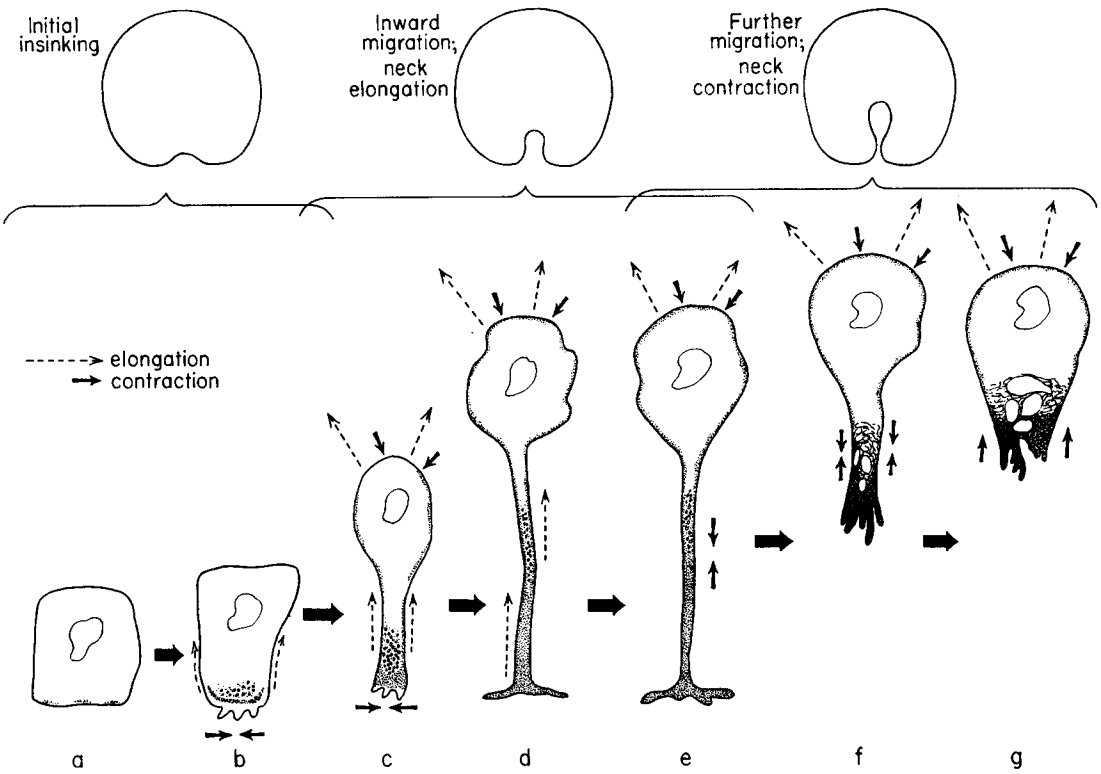

FIGURE 16 Theoretical scheme for the transformations of a blastoporal cell during gastrulation, based on the hypothesis of contraction and expansion of the dense layer. The end of the cell neck remains securely adhered to adjacent cells. (*a*) The cell as it appears on the surface prior to gastrulation. (*b*) The distal surface contracts causing initial insinking of the blastoporal pit. (*c*), (*d*) The proximal cell surface begins to migrate inward, deepening the groove; the distal surface continues to contract and the neck elongates. (*e*), (*f*), (*g*) The neck contracts after it reaches maximum elongation. This shortening, together with the pull exerted by the migrating inner ends, furthers invagination and pulls adjacent cells into the groove. Some flask cells bypass stages *d* and *e*.

FIGURE 14 Special type of cell seen among the involuting mesodermal cells at Stage 10B. (See *sm*, Fig. 8 *C*.) Part of the cell extends in a finger-like process along the surface of the blastoporal groove (*bg*); the tip of the process forms an interlocking junction (*cj*) with an extension of a similar cell. The body of the cell contains many pigment granules (*pg*) and cytoplasmic particles (*g*) in the size range of glycogen granules; *gb*, granular body; *i*, intercellular space; *l*, lipid droplets; *p*, pseudopodium-like processes; *y*, yolk platelets. × 8,000.

FIGURE 15 Higher magnification of area outlined in Fig. 14. The complex cell junction (*cj*) between the tips of two extended mesodermal cells is indicated by arrows. Microvilli (*mv*) filled with the granular matrix of the dense layer (*dl*) extend from the surface of the process facing the blastoporal groove (*bg*). Beneath the dense layer are vesicles (*v*), membranes (*m*) and cytoplasmic (glycogen ?) granules (*g*); *i*, intercellular spaces; *pg*, pigment granule. × 33,000.

microscopic study of developing amphibian ectoderm, *Roux' Arch.*, 1957, **150,** 177.

14. His, W., Unsere Körperform und das physiologische Problem ihrer Entstehung, Leipzig, 1874.
15. Holtfreter, J., Properties and functions of the surface coat in amphibian embryos, *J. Exp. Zool.*, 1943, **93,** 251.
16. Holtfreter, J., A study of the mechanics of gastrulation. Part I, *J. Exp. Zool.*, 1943, **94,** 261.
17. Holtfreter, J., A study of the mechanics of gastrulation. Part II, *J. Exp. Zool.*, 1944, **95,** 171.
18. Holtfreter, J., Structure, motility and locomotion in isolated embryonic amphibian cells, *J. Morphol.*, 1946, **79,** 27.
19. Holtfreter, J., Observations on the migration, aggregation and phagocytosis of embryonic cells, *J. Morphol.*, 1947, **80,** 25.
20. Holtfreter, J., Changes of structure and the kinetics of differentiating embryonic cells, *J. Morphol.*, 1947, **80,** 57.
21. Holtfreter, J., Significance of the cell membrane in embryonic processes, *Ann. New York Acad. Sc.*, 1948, **49,** 709.
22. Karasaki, S., Electron microscope studies on cytoplasmic structures of ectoderm cells of the *Triturus* embryo during the early phase of differentiation, *Embryologia*, 1959, **4,** 247.
23. Lehmann, F. E., Der Feinbau der Organoide bon *Amoeba proteus* und seine Beeinflussung durch verschiedene Fixierstoffe, *Ergebn. Biol.*, 1958, **21,** 88.
24. Lesseps, R. J., Cell surface projections: their role in the aggregation of embryonic chick cells as revealed by electron microscopy, *J. Exp. Zool.*, 1963, **153,** 171.
25. Lewis, W. H., Mechanics of invagination, *Anat. Rec.*, 1947, **97,** 139.
26. Lewis, W. H., Gel layers of cells and eggs and their role in early development, *Lect. Ser. Roscoe B. Jackson Mem. Lab.*, 1949, 59.
27. Løvtrup, S., On the surface coat in the amphibian embryo, *J. Exp. Zool.*, 1962, **150,** 197.
28. Luft, J. H., Improvements in epoxy resin embedding methods, *J. Biophysic. and Biochem. Cytol.*, 1961, **9,** 409.
29. Matsumoto, A., Electron microscopic observations on the cytoplasmic processes in *Triturus* embryo in early developmental stages, *J. Electronmicroscopy*, 1961, **10,** 39.
30. Niu, M. C., and Twitty, V. C., The differentiation of gastrula ectoderm in medium conditioned by axial mesoderm, *Proc. Nat. Acad. Sc.*, 1953, **39,** 985.
31. Parsons, D. F., A simple method for obtaining increased contrast in Araldite sections by using postfixation staining of tissues with potassium permangenate, *J. Biophysic. and Biochem. Cytol.*, 1961, **11,** 492.
32. Pitelka, D., Electron Microscope Study of Protozoa, New York, MacMillan Co., 1963.
33. Reynolds, E. S., The use of lead citrate at high pH as an electron-dense stain in electron microscopy, *J. Cell Biol.*, 1963, **17,** 208.
34. Rhumbler, L., Zur Mechanik des Gastrulationsvorganges, insbesondere der Invagination, *Arch. Entwcklngsmechn.*, 1902, **14,** 401.
35. Ruffini, A., Fisiogenia, Milano, F. Vallardi, 1925.
36. Schechtman, A. M., The mechanism of amphibian gastrulation, *Univ. California Pub. Zool.* 1942, **51,** 1.
37. Shumway, W., Stages in the normal development of *Rana pipiens*. I. External form, *Anat. Rec.*, 1940, **78,** 139.
38. Townes, P. L., and Holtfreter, J., Directed movements and selective adhesion of embryonic amphibian cells, *J. Exp. Zool.*, 1955, **128,** 53.
39. Vogt, W., Gestaltungsanalyse am Amphibienkeim mit örtlicher Vitafärbung. II. Teil, Gastrulation und Mesodermbildung bei Urodelen und Anuren, *Arch. Entwcklngsmechn.*, 1929, **120,** 384.
40. Waddington, C. H., Organizers and Genes, Cambridge University Press, 1940.
41. Wohlfarth-Botterman, K. E., Protistenstudien. X. Licht- und electronen-mikroskopische Untersuchungen an der Amobe *Hyalodiscus simplex* n. sp., *Protoplasma*, 1960, **52,** 58.
42. Wohlfarth-Bottermann, K. E., Cytologische Studien. VII. Strukturaspekte der Grundsubstanz des Cytoplasmas nach Einwirkung verschiedener Fixierungsmittel, *Protoplasma*, 1961, **53,** 259.
43. Wohlfarth-Botterman, K. E., Cell structures and their significance for ameboid movement, *in* International Review of Cytology, (G. H. Bourne and J. F. Danielli, editors), New York, The Academic Press, Inc., 1964.